FATIGUE CRACK INITIATION AND GROWTH OF STAINLESS STEELS IN 3%NACL SOLUTION

M. NAKAJIMA*, Y. AKATSUKA** and K. TOKAJI***

* *Department of Mechanical Engineering, Toyota College of Technology, 2-1 Eisei-cho, 471 Toyota, Japan*
** *Kai Industries Co., Ltd, 1110 Oyana, 501-32 Seki, Japan*
*** *Department of Mechanical Engineering, Gifu University, 1-1 Yanagido, 501-11 Gifu, Japan*

ABSTRACT

Corrosion fatigue tests were conducted on a duplex stainless steel, SUS329J4L, and an austenitic stainless steel, SUS304, in order to clarify the crack initiation and small crack growth behavior in 3%NaCl solution. Crack initiation occurred by ductile transgranular slip for both stainless steels in room air. On the other hand, cracks initiated at austenite-ferrite phase boundary for SUS329J4L and from corrosion pits for SUS304 in 3%NaCl solution. Fatigue crack growth in the microstructurally small region seemed to be enhanced in 3%NaCl solution for both stainless steels. In larger size region, the crack growth behavior for SUS329J4L was coincident with $da/dN - \Delta K_{eff}$ relationships of long cracks, while the breakdown in ΔK similitude was found for SUS304. Environmental effects are less evident in long cracks, except for some acceleration of da/dN at high ΔK values for both stainless steels.

KEYWORDS

Corrosion fatigue, Crack initiation, Crack growth, Small crack, Duplex stainless steel, Austenitic stainless steel, 3%NaCl solution.

INTRODUCTION

The current needs for stainless steels are high strength, good toughness and corrosion resistance. However, austenitic stainless steels with excellent corrosion resistance, *e.g.* SUS304, have a low fatigue strength and are remarkably susceptible to stress corrosion cracking (SCC) in corrosive environments including chlorine ion (Cl^-). Ferritic stainless steels, such as SUS430, have lower ductility and toughness. Martensitic stainless steels, *e.g.* SUS410, have lower corrosion resistance because of their low Cr content. On the contrary, it is known that austenitic-ferritic (duplex) stainless steels have high strength, toughness and good corrosion resistance. In duplex stainless steels, many studies have been conducted on a microstructure (Ogawa *et al.*, 1990; Marrow and King, 1994), crack growth characteristics (Fukaura *et al.*, 1986; Ogiyama *et al.*, 1984) and corrosion fatigue behavior (Amzallag *et al.*, 1978; Komai and Irifune, 1987), but fatigue crack initiation and small crack growth behavior in a corrosive environment have not been fully understood (Moskovitz and Pelloux, 1978).

In the present paper, fatigue crack initiation and small crack growth behavior in 3%NaCl solution have been studied using an improved austenitic-ferritic stainless steel, SUS329J4L, and the obtained results were compared with those of austenitic stainless steel, SUS304.

EXPERIMENTAL PROCEDURES

Materials

The materials used in this study were an austenitic-ferritic stainless steel, SUS329J4L, and an austenitic stainless steel, SUS304. The chemical compositions of both stainless steels are listed in Table 1. SUS329J4L and SUS304 were solution treated at 1050 ℃ for 15*min* and at 1100 ℃ for 30*min*, respectively.

Table 1. Chemical compositions (wt.%) of materials.

Material	C	Si	Mn	P	S	Cu	Ni	Cr	Mo	N	Fe
SUS329J4L	0.015	0.41	0.71	0.031	0.0002	0.21	6.71	25.60	3.06	0.15	Bal.
SUS304	0.05	0.46	1.33	0.031	0.003	0.39	8.21	18.25	0.28	0.08	Bal.

Table 2. Mechanical properties of materials.

Material	0.2%proof stress $\sigma_{0.2}$ MPa	Tensile strength σ_B MPa	Breaking strength on final area σ_T MPa	Elongation δ %	Reduction of area ϕ %
SUS329J4L	501	731	1625	38	77
SUS304	250	603	1766	63	80

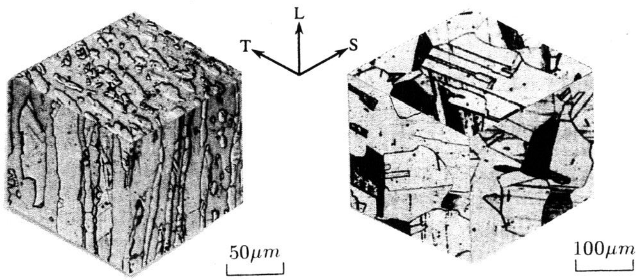

(a) SUS329J4L (b) SUS304

Fig.1. Microstructures of SUS329J4L and SUS304.

The mechanical properties after solution treatment are given in Table 2. Figure 1 shows the microstructures of both steels. The microstructure of SUS329J4L (Fig.1 (a)) contained

approximately 50% austenite (γ-phase) in volume, where austenite islands are in ferrite matrix. On the other hand, the microstructure of SUS304 is austenitic. After heat treatment specimens were machined. CT specimens (L-T direction) with 10*mm* thickness were used for long cracks, and the specimens shown in Fig.2 were for small cracks (L direction), which have a shallow notch (depth 0.4*mm*) to restrict the crack initiation site, whose stress concentration factor is about 1.05.

Fatigue Tests

Fatigue tests were conducted using electro-hydraulic testing machines at a test frequency of 10Hz in room air and 1Hz in 3%NaCl solution. Temperature, pH and dissolved oxygen content of the 3%NaCl solution were 30 ℃, 6.0 and 6.8*ppm*, respectively. Fatigue tests for long and small cracks were performed at a stress ratio of 0.05 and −1, respectively. Crack closure for long cracks was measured by an unloading elastic compliance method (Kikukawa *et al.*, 1976). Fracture surfaces were examined using an scanning electron microscope (SEM).

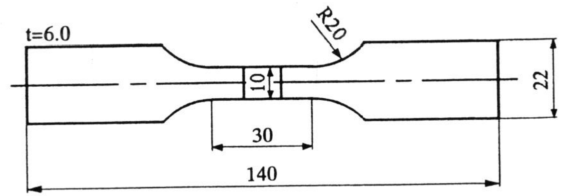

Fig.2. Specimen configuration for small cracks.

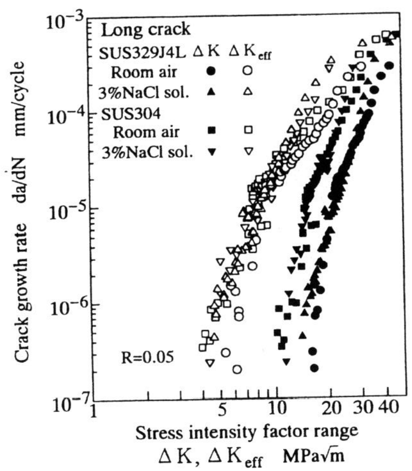

Fig.3. $da/dN - \Delta K$ and ΔK_{eff} relationships for long cracks.

RESULTS AND DISCUSSION

Growth Behavior of Long Fatigue Cracks

The relationships between crack growth rate, da/dN, and stress intensity factor range, ΔK, for long cracks ($\geq 20mm$) are shown in Fig.3. Comparing the results for both steels, the crack growth rates are lower and the threshold stress intensity is higher for SUS329J4L than SUS304 in room air and in 3%NaCl solution, indicating higher crack growth resistance in the former material. Environmental effects are less evident in both steels, except for slight acceleration of da/dN at high ΔK regime.

As can be seen in Fig.3, the difference between the $da/dN - \Delta K$ relationships almost disappears in terms of the effective stress intensity factor range, ΔK_{eff}. Thus the higher crack growth resistance of SUS329J4L can be attributed to higher crack closure level compared with SUS304. On the other hand, environmental effects are more evident, that is, enhanced da/dN is observed at $\Delta K_{eff} \geq 12\text{MPa}\sqrt{\text{m}}$ for both steels.

Crack Initiation Behavior

Figure 4 (a) and (b) show fractographs of the crack initiation sites for SUS329J4L in room air and 3%NaCl solution, respectively. Ductile transgranular facet whose size is several tens of micron on the surface is observed at the crack initiation site as shown in Fig.4 (a). Based on many studies performed on austenitic-ferritic stainless steels, the crack initiation sites depend on stress level, environment, alloy composition and microstructure (Moskovitz and Pelloux, 1978; Fukaura *et al.*, 1986). In the present result, the persistent slip bands prior to crack initiation were observed, subsequently cracks initiated. Since the morphology of the transgranular facet is similar to that of α-phase in a previous study (Ogawa *et al.*, 1990), it is considered that the crack initiation occurred by slip in α-phase. Furthermore, fracture surface surrounding the crack initiation site is ductile in room air. The crack initiation in 3%NaCl solution occurred at austenite-ferrite phase boundary, as can be seen in Fig.4 (b), and the morphology of fracture surface near the crack initiation site is irregular and brittle.

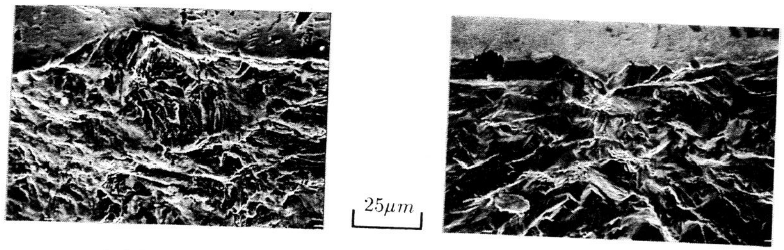

(a) Room air (b) 3%NaCl sol.

Fig.4. Microscopic views of crack initiation site for SUS329J4L.

Fractographs of the crack initiation sites for SUS304 in room air and in 3%NaCl solution are shown in Fig.5 (a) and (b), respectively. Ductile transgranular facet is observed at the crack initiation site in room air, as shown in Fig.5 (a). Persistent slip bands also developed prior to crack initiation. The morphology around the crack initiation site is

relatively flat and ductile. On the other hand, as can be seen in Fig.5 (b) the crack was generated from a corrosion pit whose size is about $8\mu m$ in depth. However, it is found in SUS304 that cracks were also generated from the sites other than corrosion pit. The stress intensity factor, K, of the corrosion pit shown in Fig.5 (b) was calculated by regarding it as a crack. The obtained K value is $0.57\text{MPa}\sqrt{\text{m}}$, which is in the range of the K values, $0.37\sim1.40\text{MPa}\sqrt{\text{m}}$, obtained in a previous study for SUS304, (Nakajima and Tokaji, 1996). Fracture surface around the crack initiation site reveals relatively brittle feature. In addition, the environmental acceleration for crack initiation was not observed for both stainless steels in the present study.

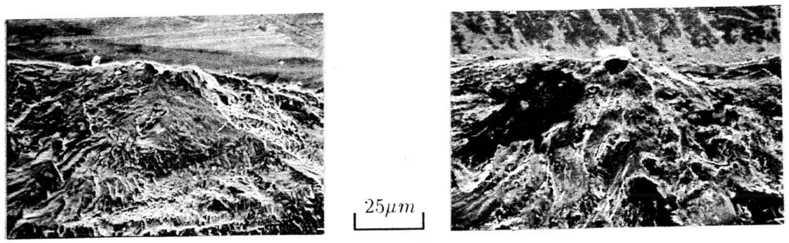

(a) Room air (b) 3%NaCl sol.

Fig.5. Microscopic views of crack initiation site for SUS304.

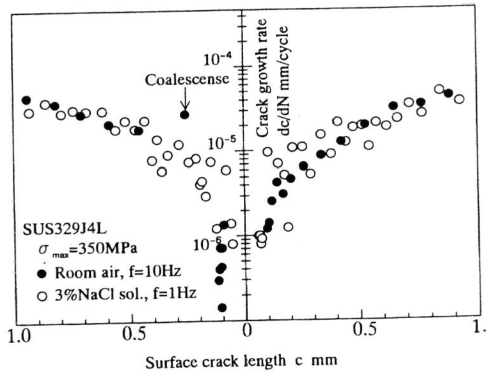

Fig.6. Relationships between dc/dN and c for SUS329J4L.

Early Growth of Small Fatigue Cracks

Figure 6 shows the relationships between crack growth rate, dc/dN, and crack length on the specimen surface, c, for SUS329J4L. Since early crack growth immediately after the crack initiation is influenced by microstructure, the variation of dc/dN in the region of crack size below $200\mu m$ is remarkable. As shown in Fig.1 (a), the dual-phase microstructure of SUS329J4L contains austenite islands in ferrite matrix, where the width of austenite islands is $15\sim20\mu m$. It is known that the austenite-phase retards crack propagation (Moskovitz and Pelloux, 1978), and thus when small cracks propagate across the dual-phase boundaries, the variation of dc/dN occurs. Therefore, cracks smaller than $200\mu m$ can be considered as the microstructurally small cracks.

Moreover, in this region, dc/dN increases rapidly and the rates in 3%NaCl solution are slightly faster than those in room air. The rates in both environments are almost the same above this region. Based on these results and SEM micrographs (Fig.4 (a) and (b)), it is suggested that the crack growth in the microstructurally small region is enhanced by 3%NaCl solution. In larger size region, environmental effects are less evident.

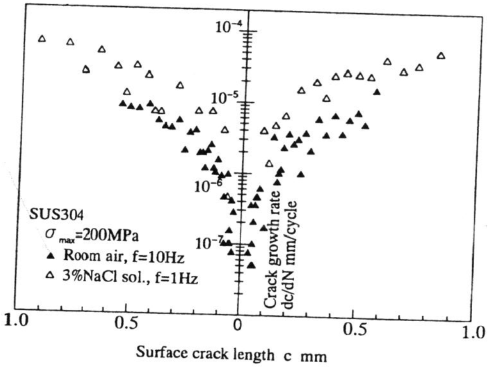

Fig.7. Relationships between dc/dN and c for SUS304.

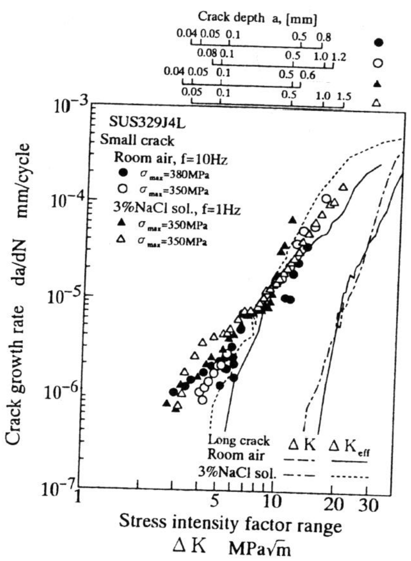

Fig.8. $da/dN - \Delta K$ relationships of small cracks for SUS329J4L.

The relationships between dc/dN and c for SUS304 are shown in Fig.7. The variation of dc/dN in the region of crack size below $500\mu m$ is less remarkable as compared to SUS329J4L. It is considered that this behavior is caused by the single-phase microstructure of SUS304. Furthermore, in the region of crack size below $500\mu m$ the rates in 3%NaCl solution are clearly faster than those in room air, indicating that also in SUS304 the crack growth in the small size region immediately after the crack initiation is enhanced by 3%NaCl solution. Environmental effects in this region are more evident than SUS329J4L.

Growth Behavior of Small Fatigue Cracks

Figure 8 shows the $da/dN - \Delta K$ relationships of small cracks for SUS329J4L. For comparison, data of long cracks are also represented by lines in the figure. The stress intensity factor of small surface cracks was calculated using an analytical solution developed by Newman and Raju (Newman, 1979). Comparing with the results of long cracks, the $da/dN - \Delta K$ relationships of small cracks coincide with the $da/dN - \Delta K_{eff}$ relationships of long cracks at the region of $\Delta K_{eff} \geq 8\mathrm{MPa}\sqrt{\mathrm{m}}$, irrespective of environment. On the other hand, da/dN of small cracks accelerates in the region of $\Delta K_{eff} \leq 8\mathrm{MPa}\sqrt{\mathrm{m}}$ in both environments. Furthermore, the rates in 3%NaCl solution seem to be slightly faster than those in room air.

The $da/dN - \Delta K$ relationships of small cracks for SUS304 are shown in Fig.9. The lines in the figure represent long crack data for comparison. As can be seen in the figure, the growth rates of small cracks depend on stress level, indicating the breakdown in ΔK similitude due to large scale yielding condition, because stress level of 200MPa is relatively high compared to the proof stress of 250MPa, as shown in Table 2. The use of ΔK is inappropriate for small cracks of SUS304, but the environmental effects seem to be evident.

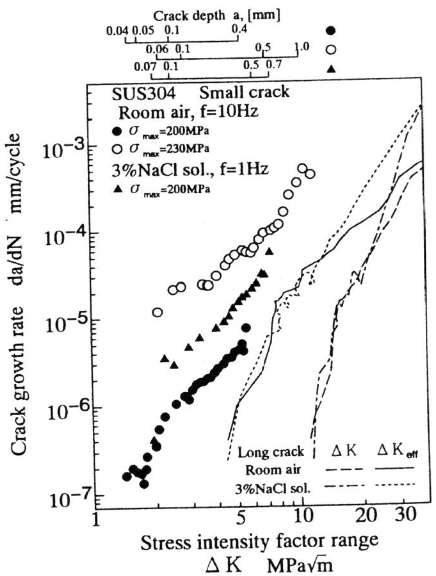

Fig.9. $da/dN - \Delta K$ relationships of small cracks for SUS304.

CONCLUSIONS

Fatigue tests were conducted on two kinds of stainless steels, *i.e.* a duplex stainless steel, SUS329J4L, and an austenitic stainless steel, SUS304, in order to clarify the crack initiation and small crack growth behavior in 3%NaCl solution. The conclusions obtained are as follows;

(1) Crack initiation occurred by ductile transgranular slip for both stainless steels in room air. On the other hand, crack initiated at austenite-ferrite phase boundary for SUS329J4L and from corrosion pit for SUS304 in 3%NaCl solution.

(2) Fatigue crack growth in the microstructurally small region was slightly enhanced in 3%NaCl solution for both stainless steels.

(3) In larger crack size region, the crack growth behavior for SUS329J4L was coincident with the $da/dN - \Delta K_{eff}$ relationships of the long cracks. On the other hand, the breakdown in ΔK similitude was observed for SUS304.

(4) Environmental effects are less evident in long cracks, except for some acceleration of crack growth rates at high ΔK regime for both stainless steels.

REFERENCES

Amzallag,C., P.Rabbe and A.Desestret (1978). Corrosion-fatigue behavior of some special stainless steels. In: *ASTM STP 642*, 117-132.

Fukaura,K., H.Izumi and H.Kawabe (1986). Microscopic study of initial fatigue cracks in two-phase stainless steel. *J.of Soc.Mater.Sci., Jpn.*, **35**, 610-616. (in Japanese)

Kikukawa,M., M.Jono, K.Tanaka and M.Takatani (1976). Measurement of fatigue crack propagation and crack closure at low stress intensity level by unloading elastic compliance method. *J.of Soc.Mater.Sci., Jpn.*, **25**, 899-903. (in Japanese)

Komai,K., and K.Irifune (1987). Corrosion fatigue crack growth behavior of dual-phase stainless steel in synthetic sea water. *J.of Soc.Mater.Sci., Jpn.*, **36**, 141-146. (in Japanese)

Marrow,T.J. and J.E.King (1994). Microstructural and environmental effects on fatigue crack propagation in duplex stainless steel. *Fatigue Fract. Engng Mater. Struct.*, **17**, 761-771.

Moskovitz,J.A. and R.M.Pelloux (1978). Corrosion-fatigue behavior of austenitic-ferritic stainless steels. In: *ASTM STP 642*, 133-154.

Nakajima,M., and K.Tokaji (1996). A mechanical condition of fatigue crack initiation from corrosion pits. *Proceeding of Fatigue 96*, (in press).

Newman,J.C.,Jr., (1979). A review and assessment of the stress-intensity factors for surface cracks. In: *ASTM STP 687*, 16-42.

Ogawa,T., K.Tokaji and Y.Kato (1990). Growth characteristics of large and small fatigue cracks in dual-phase stainless steel. *Trans.Jpn.Soc.Mech.Eng.*, **56(A)**, 752-758. (in Japanese)

Ogiyama,H., H.Tsukuda, Y.Soyama and I.Tamura (1984). Fatigue crack growth behavior of austenite-ferrite two-phase iron alloy. *J.of Soc.Mater.Sci., Jpn.*, **33**, 1059-1064. (in Japanese)